Chemical Kinetics of Ethanol Oxidation

Juan Li[1], Andrei Kazakov[2], Frederick L. Dryer[2*]
[1]Praxair, Inc.
Tonawanda, NY 14150, USA
[2]Department of Mechanical and Aerospace Engineering
Princeton University
Princeton, NJ 08544, USA

Abstract
Experimental profiles of stable species mole fractions are reported for ethanol oxidation in a Variable Pressure Flow Reactor (VPFR) at initial temperatures of 800-950K and constant pressures of 3 to 12atm. A detailed mechanism for ethanol combustion is developed in a hierarchical manner, and at each level, the newly added portions of the mechanism are tested by thorough comparison of model predictions and experimental results found in laminar premixed flames, shock tubes, and flow reactors. The present ethanol mechanism predicts reasonably well the major species profiles of the VPFR oxidation experiments, and significantly improves the predictions of the experimental targets originally investigated by a most recent ethanol mechanism [1].

Introduction

Ethanol (C_2H_5OH) is a very important energy carrier that can be produced from renewable energy resources. It can be used as a fuel extender, octane enhancer, and oxygen-additive in, or as an alternative, neat fuel to replace reformulated gasoline. Ethanol also has potential as a hydrogen carrier for fuel cell applications. The 1990 Clean Air Act Amendments [2] presently require the addition of oxygenates to reformulated gasoline, with seasonal adjustments, on the premise that oxygen content decreases automotive emissions, particularly smog generation participants and carbon monoxide. Ethanol is favored to replace methyl tertiary butyl ether (MTBE), another widely used oxygenate additive that has become unpopular based upon ground water contamination and human health effects. While most ethanol is currently generated by fermentation (grain alcohol), recent developments suggest that ethanol fuel can be derived more efficiently from other biomass, thus offering potential to reduce dependence on fossil fuel energy resources.

The chemistry of gas-phase oxidation and pyrolysis of ethanol have been the subjects of numerous studies over the last five decades. Data have been reported from shock tubes, static reactors, flow reactors, diffusion flames, and laminar premixed flame experiments. Norton and Dryer [3] conducted a series of ethanol oxidation experiments in an Atmospheric Pressure Flow Reactor (APFR). In the modeling efforts of Norton and Dryer, as well as those of several other investigators [4,5] emphasized the importance of including all three isomeric forms of C_2H_5O produced by H-atom abstraction from ethanol. More recently, Marinov [1] carried out an extensive detailed kinetic modeling study of ethanol combustion at intermediate and high temperatures. His computational results indicated that ethanol oxidation exhibits strong sensitivity to branching ratio assignments of the H-atom abstraction reactions of ethanol as well as to the kinetics of its unimolecular decomposition. The mechanism performed reasonably well under the experimental conditions found in laminar premixed flames, shock tubes, and the APFR. However, few experiments to validate the pyrolysis and high-pressure oxidation characteristics of ethanol at flow reactor conditions were available for comparison. In recently published works [6,7], our laboratory has produced new pyrolysis data, and new rate determinations for ethanol uni-molecular decomposition reactions.

The present paper reports new flow reactor data of ethanol oxidation at high-pressure conditions (3-12atm with initial temperatures of 800-950K). Since the Marinov mechanism does not predict well either the earlier pyrolysis or the new oxidation data, a revised, new detailed oxidation mechanism was developed. The mechanism is described and compared here with a wide range of experimental data, including the present high-pressure flow reactor results, shock tube ignition delay data, and laminar flame speed measurements.

Experimental Methods

Experiments were conducted in the Princeton Variable Pressure Flow Reactor (VPFR). A schematic of the flow reactor is shown in Figure 1. Detailed information about the VPFR instrumentation and experimental methodology can be found in other

* Corresponding author: fldyer@princeton.edu
Associated Web site: http://www.princeton.edu/~combust
Proceedings of the European Combustion Meeting 2005

publications [8,9], and only a brief description of these issues is given here.

Carrier gas (N_2 in this study) is heated by a pair of electrical resistance heaters and directed into a reactor duct. Oxygen is also introduced at the duct entrance. The carrier gas/oxygen mixture flows around a baffle plate into a gap serving as the entrance to a diffuser. The vaporized fuel (ethanol) flows into the center tube of a fuel injector, and injected radially outward into the gap where it rapidly mixes with the carrier gas and oxygen. The reacting mixture exits the diffuser into a constant area test section. Near the exit of the test section, a sampling probe is positioned on the reactor centerline to continuously extract and convectively quench a small portion of the flow. At the same axial location, the local gas temperature is measured with a type R thermocouple.

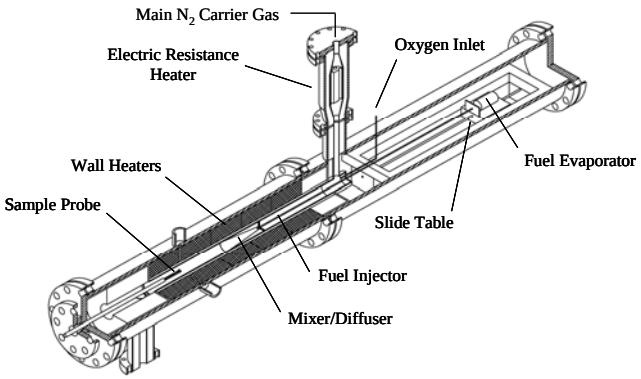

Figure 1. Schematic of the variable pressure flow reactor.

The sample gas flows via heated Teflon lines to analytical equipments including a Fourier transform infrared spectrometer (FTIR), an electrochemical O_2 analyzer, and a pair of non-dispersive infrared analyzers for CO and CO_2. The majority of the stable species of interest (C_2H_5OH, H_2O, C_2H_4, CH_4, CH_3CHO, etc.) are measured continuously on-line using FTIR spectrometry. The measurement uncertainties for the data reported here are: O_2 - ±2%, CO - ±2%, CO_2 - ±2%, C_2H_5OH - ±3%, H_2O - ±6%, C_2H_4 - ±3%, CH_4 - ±4%, CH_3CHO - ±3%, CH_2O - ±3%, C_2H_6 - ±4%, and C_2H_2 - ±3% of reading. Additional species can be determined using discrete gas samples acquired from the sample flow and off-line gas chromatographic analyses.

The distance between the point of fuel injection and the sampling position is varied by moving the fuel vapor injector probe (with attached mixer/diffuser assembly), relative to the fixed sampling location. Mean axial velocity measurements along the centerline of the reactor are used to correlate distance with residence time. In this way, profiles of stable species versus the residence time can be determined experimentally.

A series of species-time history ethanol oxidation experiments were conducted in the VPFR at initial temperatures of 800-950K and pressures of 3-12atm with equivalence ratio from 0.6 to 1.4. Figures 2-3 present experimental species time history profiles for two representative cases at 3 and 9atm, respectively. In all of the experiments, the total carbon and oxygen balances experimentally determined at each residence time were within 5% of the specified input. The steady total carbon and oxygen concentrations at each sampling location not only provide verification of the experimental measurements, but also imply that any other carbon- or oxygen-containing stable species are present in negligible quantities. This result was also verified by off-line gas chromatographic analyses.

Chemical Kinetics Model

Predictions using the ethanol mechanism of Marinov [1] are compared with the present experimental data at 3 and 9 atm pressure in Figures 2 and 3. The model predictions are compared to the experimental measurements by shifting the simulated values along the time axis to match the 50% fuel consumption point. The predicted fuel and oxygen consumption rates, as well as the production rates of major intermediates, such as H_2O, CH_4, and C_2H_4 are substantially different from the experiment results, independent of any time shifting considerations.

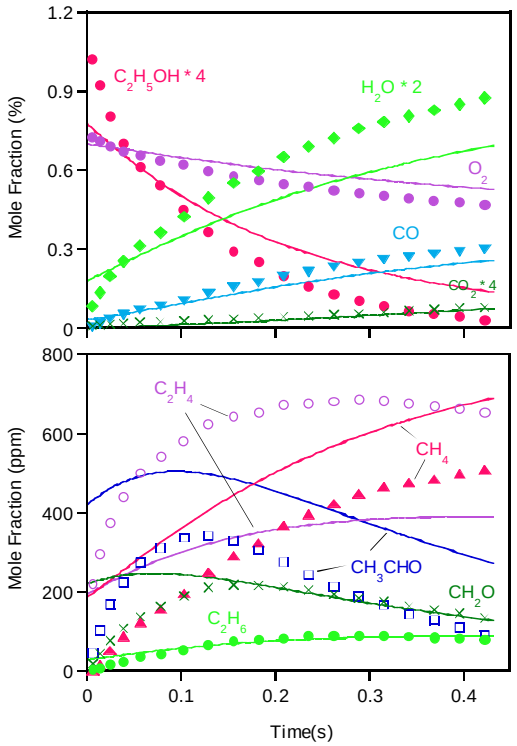

Figure 2. Reaction profiles of $C_2H_5OH/O_2/N_2$ mixture in the VPFR. Initial conditions: C_2H_5OH = 0.30%, ϕ = 1.2 with balance N_2 at 3.0atm and 950K. Symbols: present experiment data; lines: predictions of Marinov model [1].

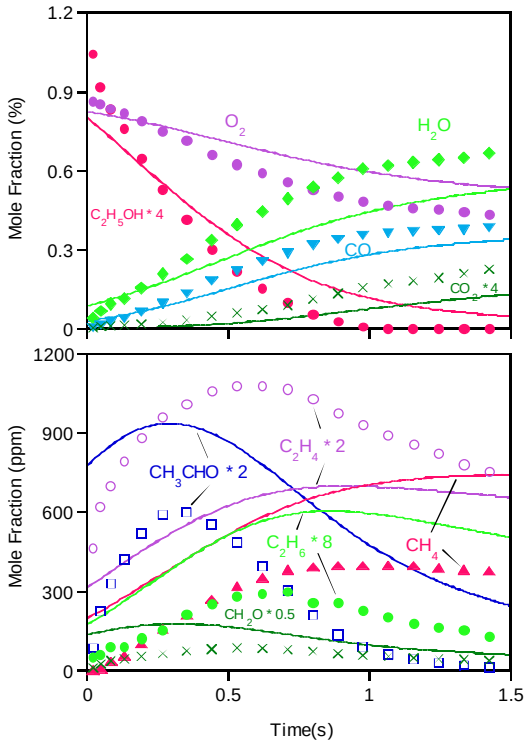

Figure 3. Reaction profiles of $C_2H_5OH/O_2/N_2$ mixture in the VPFR. Initial conditions: C_2H_5OH = 0.30%, ϕ = 1.0 with balance N_2 at 9atm and 830K. Symbols: present experiment data; lines: predictions of Marinov model [1].

To better simulate the new observations, a new, revised detailed mechanism for ethanol pyrolysis and oxidation was developed, consisting of 39 species and 228 reversible elementary reactions. The detailed mechanism was developed in a hierarchical manner. The combustion of hydrocarbon species follows a basic series steps, beginning with initiation decomposition reactions, followed by radical attack on the fuel, production of generally smaller intermediates, and finally a chain of aldehyde $\rightarrow$ CO $\rightarrow$ CO_2 steps. In the above process, the radical pool responsible for chain propagation, branching, and termination is mainly determined by the H_2/O_2 reaction mechanism. By taking these basic steps in the reverse order, the detailed mechanism was built up hierarchically. The present ethanol mechanism starts from the H_2 submechanism, followed by C_1 subsets including those for CO, CH_2O, CH_3OH, and CH_4 combustion, then C_2 portion including the reactions for C_2H_X (X = 1–6), CH_3CHO, and C_2H_5OH. The hierarchy of the development of the ethanol chemical kinetics model is shown in Figure 4.

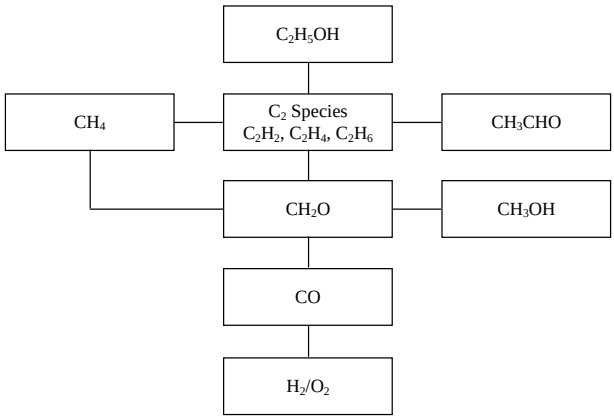

Figure 4. Hierarchical structure of the present ethanol oxidation mechanism.

At each level, the newly added portions of the mechanism were tested and validated by thorough comparison with experimental data over wide ranges of physical conditions for the sub-mechanism species. These experimental sources included laminar flame speeds, shock tube ignition delay data, flow reactor measurements, and other sources such as observations in static and stirred reactors. In conjunction with sensitivity and reaction flux analyses, the selected starting sub-mechanisms (H_2/O_2 mechanism of Mueller et al. [9], CH_3OH/O_2 mechanism of Held and Dryer [10], and C_2H_5OH/O_2 mechanism of Marinov [1]), were updated and/or revised to reflect recent publications of thermodynamic data, rate coefficients, and channel results. Detailed information of each level of the present ethanol mechanism development can be found in reference 11, and only a brief description is given below.

1. H_2/O_2 sub-mechanism. The entire sub-mechanism was replaced with our recent updated version [12] of that published earlier by Mueller et al [9]. The revised mechanism encompasses recently published thermodynamic data of OH and rate constants of the two important reactions, H + O_2 = OH + O [13] and H + O_2 (+M) = HO_2 (+M) [14]. Sensitivity analyses shows that the reaction H + OH + M = H_2O + M is of significance to the observations in the high-pressure flames propagation. Its rate constant was modified within its known uncertainty limits to achieve flame propagation model performance.

2. CO, CH_2O, CH_3OH/O_2 sub-mechanism. The C_1 sub-mechanism was developed based on the CH_3OH/O_2 mechanism of Held and Dryer [10]. Recently, kinetic parameters for CH_3, HCO, and CH_2O related reactions as well as new experimental data for C_1 species have become available. The CO/O_2, CH_2O/O_2, and CH_3OH/O_2 mechanisms were revisited, considering the new kinetic information. The most important revisions to the original model involve the rate constant descriptions for the reactions CO + OH = CO_2 + H and HCO + M = H +

CO + M. Recent theoretical calculations of the rate constant of CO + OH = CO_2 + H predict values higher than experimental measurements at low to intermediate temperatures [11]. The temperature-dependent sensitivity analysis of Zhao et al. [15] demonstrates that flame speeds of hydrocarbons are most sensitive to the value of the rate constant of HCO + M = H + CO + M at 1300–2000K, well above the range of conditions of the recently published measurement for this reaction. In the present study, a weighted least square fitting of literature data was adopted, resulting the rate constant expressions of $k=2.23\times10^{5}T^{1.89}\exp(-\frac{583}{T})$ and $k=4.75\times10^{11}T^{0.66}\exp(-\frac{7485}{T})$ for these two reactions, respectively.

3. C_2H_X /O_2 sub-mechanism. The C_2H_X (X = 1–6), as well as CH_2 and HCCO sub-models were primarily taken from the C_2 chemistry of Wang et al. [16], which was derived from GRI-1.2 mechanism [17]. Wang et al tested their mechanism against a variety of C_2H_2 and C_2H_4 experiments, including ignition behavior, laminar flame propagation, and detailed structure of burner-stabilized flames, and the mechanism was demonstrated to reproduce most of the experiment results.

4. CH_3CHO/O_2 sub-mechanism. The acetaldehyde combustion chemistry, including CH_3CHO, CH_3CO, CH_2CHO, and CH_2CO reactions, was based on the sub-mechanism appearing in Marinov [1]. All acetaldehyde mechanisms currently available in literature (e.g. [1], [18], [19]) failed to give reasonable predictions of acetaldehyde experiments previously conducted in the VPFR [20]. The discrepancy makes clear that considerable work remains to reconcile predictions with experimental measurements. Here we made revisions to elementary acetaldehyde reactions based on extensive literature review, especially the abstraction reactions involving OH. Further studies on the acetaldehyde decomposition and abstraction reactions with other radicals, like HO_2, are continuing.

5. C_2H_5OH/O_2 sub-mechanism. The ethanol subset consists of ethanol decomposition reactions, abstraction reactions generating three isomers of C_2H_5O due to the three different sites of abstracted H atom in C_2H_5OH molecules, and subsequent reactions of C_2H_5O to produce C_1 or other C_2 species whose mechanism has been established above. The current ethanol sub-mechanism was based on that of Marinov [1] with revisions to ethanol decomposition and abstraction reactions. The fall-off kinetics of ethanol decomposition was described by our recent study based on pyrolysis experiments with radical trappers and RRKM/master equation calculations [7]. Extensive literature review of ethanol abstraction reactions shows there are very few elementary experimental measurements available. In the present study, the rate constants of abstraction reactions were modified to better reproduce the VPFR experiments [11].

6. Thermodynamic data. The thermodynamic properties of the species in the detailed mechanism were primarily obtained from the CHEMKIN thermodynamic database [21], except for OH, HO_2, and CH_2OH. The standard heats of formation of OH and HO_2 at 298 K were updated to 8.9 kcal/mol [22] and 3.0 kcal/mol [23], respectively. The thermochemical properties of CH_2OH, including enthalpy of formation, standard entropy, and heat capacity at different temperatures, were taken from reference 24.

Results and Discussion

The ethanol mechanism described above was compared against the present VPFR experiments, and the results are shown in Figures 5 and 6. The predictions of the major stable species (C_2H_5OH, O_2, H_2O, and CO) using the present mechanism agree very well with the experimental measurements and represent a significant improvement over predictions using the Marinov mechanism [1]. For other stable species, the model predictions are reasonable but can be further improved. Mechanistic elements, particularly those involving acetaldehyde and its reactive intermediates, remain under consideration in further improving the present version of the ethanol oxidation mechanism.

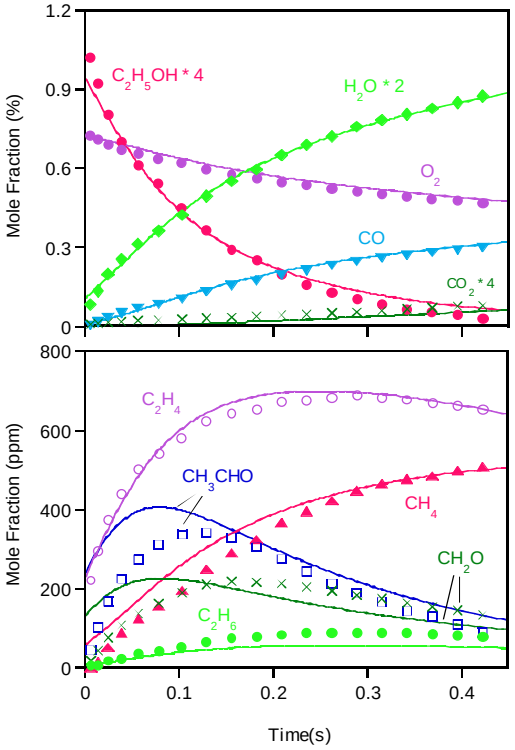

Figure 5. Reaction profiles of $C_2H_5OH/O_2/N_2$ mixture in the VPFR. Initial conditions: the same as in Figure 2. Symbols: present experiment data; lines: predictions of the present model.

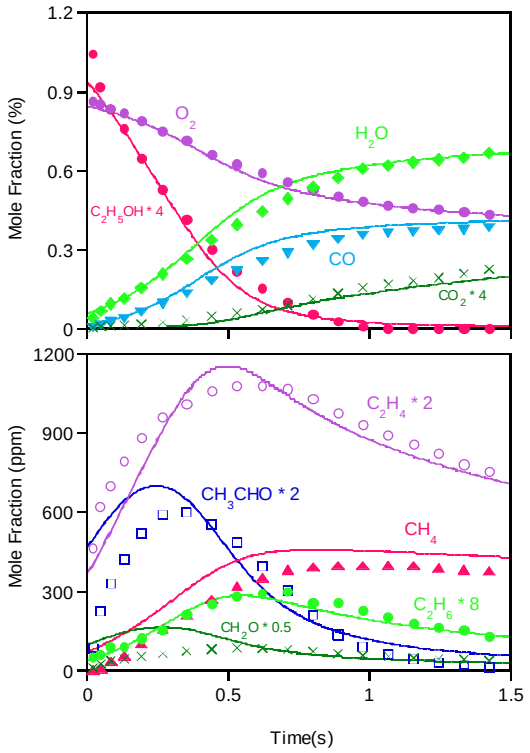

Figure 6. Reaction profiles of $C_2H_5OH/O_2/N_2$ mixture in the VPFR. Initial condition: the same as in Figure 3. Symbols: present experiment data; lines: predictions of the present model.

The present ethanol mechanism was also tested against experimental observations found in shock tubes, laminar premixed flames, and stirred reactors, with representative test results shown in Figures 7 and 8. The SENKIN [25] and PREMIX [26] codes were used for ignition delay and laminar flame speed calculations, respectively. The standard CHEMKIN transport package was used for the flame speed calculations with Soret effects and multi-component diffusion included. About 600 grid points were imposed in the PREMIX calculation to obtain fully converged laminar flame speed predictions.

The predictions of the shock tube ignition delay time of $C_2H_5OH/O_2/AR$ mixtures are presented in Figure 7. As can be seen, the predictions deviate from the experiment results by amounts comparable to those predictions obtained using [1]. Figure 8 compares the model predictions with the laminar flame speed measurement of C_2H_5OH/air mixtures at temperatures ranging from 363 to 453K. Predictions of laminar flame speed are significantly improved over those obtained with the Marinov mechanism [1].

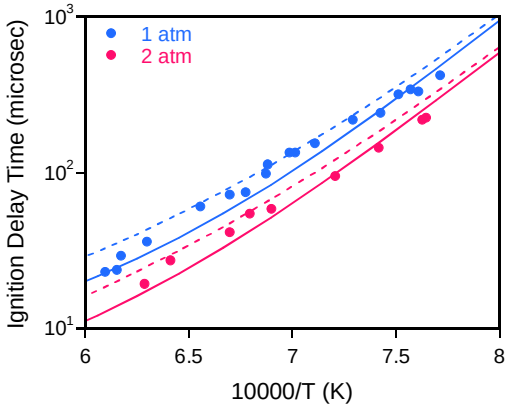

Figure 7. Ignition delay time of $C_2H_5OH/O_2/Ar$ mixture at 1 and 2atm. Initial conditions: C_2H_5OH = 1.43%, ϕ = 0.5. Symbols: experiment data [4]; dashed lines: predictions of Marinov model [1]; solid lines: predictions of the present model.

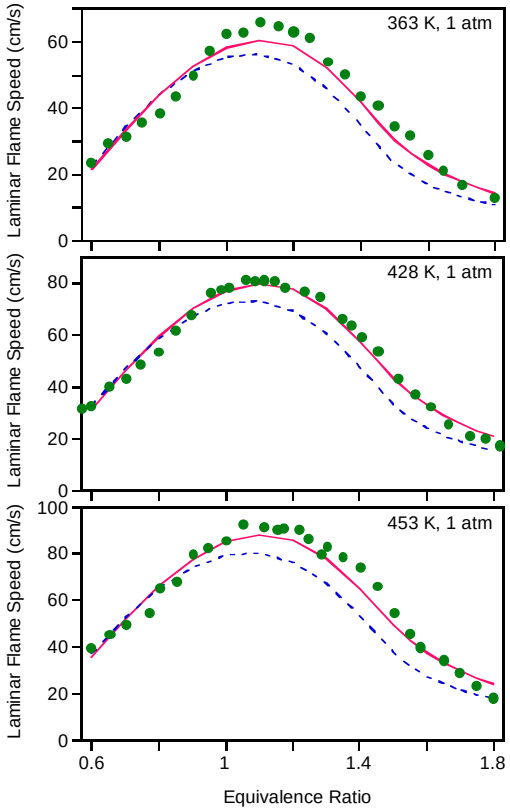

Figure 8. Atmospheric laminar flame speed of C_2H_5OH/air mixture at different initial temperature (363, 428, and 453K). Symbols: experiment data [27], dashed lines: predictions of Marinov model [1]; solid lines: predictions of the present model.

Conclusions

The first sets of high-pressure flow reactor experiments of ethanol oxidation (800-950K and 3-12atm) were performed in a VPFR to measure the time history of stable species concentrations. These

experiments provide detailed kinetics information for the development and validation of the ethanol mechanism. Predictions of the new experiments based upon a recently published ethanol oxidation mechanism [1] are significantly deficient. A new detailed mechanism for ethanol combustion was developed in a hierarchical manner, beginning with the H_2/O_2 reaction mechanism, and subsequently constructed by encompassing C_1/O_2, C_2H_X/O_2, CH_3CHO/O_2, and C_2H_5OH/O_2 subsets in order of increasing complexity. At each level, the newly added portions of the mechanism were tested by thorough comparison between numerically predicted and experimentally observed results found in laminar premixed flames, shock tubes, and flow reactors. In conjunction with sensitivity and reaction flux analyses, important updates/modifications to the original mechanisms were made to reflect recent updates of thermodynamic data, rate coefficients, and branching ratios. The present ethanol mechanism predicts reasonably well the major species profiles observed in the new VPFR experiments, and significantly improves the agreement with the experimental targets originally investigated by Marinov [1]. The present study also demonstrates the continual need to re-evaluate any "comprehensive" mechanism [28] as new experimental validation constraints are considered and/or as improved kinetic and thermochemical parameters become available.

Acknowledgements

This work was supported by the Chemical Sciences, Geosciences and Biosciences Division, Office of Basic Energy Sciences, Office of Science, U.S. Department of Energy under Grant No. DE-FG02-86ER13503. The authors also thank Mr. Paul Michniewicz for his assistance in performing the experiments.

References

1. N. M. Marinov, Int. J. Chem. Kinet., 1999, 31, 183.
2. Energy Information Administration, Alternatives to Traditional Transportation Fuels 1996, DOE/EIA-0585.
3. T. S. Norton, and F. L. Dryer, Int. J. Chem. Kinet., 1992, 24, 319.
4. K. Natarajan and K. A. Bhaskaran, Thirteenth International Shock Tube Symposium, Niagara Falls, 1981, p 834.
5. M. P. Dunphy and J. M. Simmie, J. Chem. Soc. Faraday Trans., 1991, 87, 1691; and 1991, 87, 2549.
6. J. Li, A. Kazakov, and F. L. Dryer, Int. J. Chem. Kinet. 2001, 133, 859.
7. J. Li, A. Kazakov, and F. L. Dryer, J. Phys. Chem. A 2004, 108, 7671.
8. T. J. Held, Ph.D. thesis, Department of Mechanical and Aerospace Engineering, Princeton University, Princeton, NJ, 1993.
9. M. A. Mueller, T. J. Kim, R. A. Yetter, and F. L. Dryer, Int. J. Chem. Kinet., 1999, 31, 113.
10. T. J. Held, and F. L. Dryer, Int. J. Chem. Kinet., 1998, 30, 805.
11. J. Li, Ph.D. thesis, Department of Mechanical and Aerospace Engineering, Princeton University, Princeton, NJ, 2004.
12. J. Li, Z. Zhao, A. Kazakov, and F. L. Dryer, Int. J. Chem. Kinet., 2004, 36, 566.
13. J.P. Hessler, J. Phys. Chem. A, 1998, 102, 4517.
14. J.V. Michael, M.C. Su, J.W. Sutherland, J.J. Carroll, and A.F. Wagner, J. Phys. Chem. A, 2002, 106, 5297.
15. Z. Zhao, J. Li, A. Kazakov, and F.L. Dryer, Int. J. Chem. Kinet. 2004, in press.
16. H. Wang, A. Laskin, Z. M. Djurisic, C. K. Law, S. G. Davis, and D. L. Zhu, Eastern States Section of the Combustion Institute Fall Technical Meeting, Raleigh, NC, October 1999.
17. M. Frenklach, H. Wang, M. Goldenberg, G.P. Smith, D.M. Golden, C.T. Bowman, R.K. Hanson, W.C. Gardiner, and V. Lissianski, GRI Technical Report No. GRI-95/0058, 1995.
18. A.A. Borisov, V.M. Zamanskii, A.A. Konnov, V.V. Lisyanskii, S.A. Rusakov, and G.I. Skachkov, Sov. J. Chem. Phys., 1989, 4, 2561.
19. P. Dagaut, M. Reuillon, D. Voisin, M. Cathonnet, M. McGuinness, and J.M. Simmie, Combust. Sci. and Tech. 1995, 107, 301.
20. D.C Zarubiak, Master thesis, Department of Mechanical and Aerospace Engineering, Princeton University, Princeton, NJ, 1997.
21. R. J. Kee, F. M. Rupley, and J. A. Miller, Sandia National Laboratories Report No. SAND87-8215, 1987.
22. B. Ruscic, A. F. Wagner, L. B. Harding, R. L. Asher, D. Feller, D. A. Dixon, K. A. Peterson, Y. Song, X. Qian, C. Ng, J. Liu, W. Chen, and D. W. Schwenke, J. Phys. Chem. A, 2002, 2727.
23. A. J. Hills, and C. J. Howard, J. Chem. Phys., 1984, 81, 4458.
24. R.D. Johnson III and J.W. Hudgens, J. Phys. Chem., 1996, 100, 19874.
25. A. E. Lutz, R. J. Kee, and J. A. Miller, Sandia National Laboratories Report No. SAND87-8248, 1987.
26. R. J. Kee, J. F. Grcar, M. D. Smooke, and J. A. Miller, Sandia Laboratories Report No. SAND85-8240, 1985.
27. F. N. Egolfopoulos, D. X. Du, and C. K. Law, 24th Symp. (Int.) on Combust., The Combustion Institute, Pittsburgh, 1992, p 833.
28. C. K. Westbrook, and F. L. Dryer, Combust Sci. Tech., 1979, 20, 125.